MICROMECHANISMS OF CLEAVAGE FRACTURE IN THE HAZ OF C-MN COMMERCIAL STEEL WELD

C. Moya-Gutiérrez, A. Martín-Meizoso, I. Ocaña-Arizcorreta
CEIT, Centro de Estudios e Investigaciones Técnicas de Guipúzcoa
Paseo de Manuel Lardizábal, 15, 20018 San Sebastián, Spain
cmoya@ceit.es, ameizoso@ceit.es, iocana@ceit.es

Abstract

Cleavage fracture of potentially ductile polycrystalline materials (e.g. b.c.c metals) most frequently occurs by the dynamic propagation of microcracks originated by slip-induced cracking of brittle second phase particles or inclusions Kim *et al.* [1].

The "weakest link" model has been used, which takes account the presence of three independent distributions of structural elements (particles: carbides and pearlite constituents; and a matrix: bainite packets), characterized by a crack arrest capability well over the crack propagation resistance of the cleavage planes of the crystalline lattices at three phases.

Microstructural measurements have been carried out to validate this model ,using welds with different C and Mn contents. Three point bend samples have been machined and precracked in fatigue. Fracture tests have been made at low temperatures in cleavage fracture conditions to obtain the plain strain fracture thoughness K_{IC} of the heat affected zone.

Introduction

Carbon-manganese (C-Mn) weld metals are used widely in fabricated steel structures. A particular application is in offshore constructions, for example, in the North Sea. In such rigorous conditions, it is essential to maintain good weld-metal toughness at temperatures of -20ºC or even lower. In particular, failure by cleavage, which gives rise to low fracture-toughness values, must be avoided Tweed and Knott [2].

The heat-affected zone (HAZ) of a weld is generally the weakest part and is crucial in the failure of steel structures. The reason of that is its heterogeneous microstructure owing to the sensitive variation with the thermal cycle experienced during welding.

The purpose of the work, reported here, is to develop a probabilistic model for brittle failure prediction from the HAZ of the C-Mn weld based on microstructural information.

Experimental Procedure

A low C weld steel has been utilized for experiments having the chemical composition shown in Table 1. The sample was laminated before the welding process (SAW). The welding parameters were V = 30 V, I = 90 A, speed = 405 mm/min. and energy arc = 4 kJ/mm. The pre-heating temperature was 20º C. The steel was supplied by Corus Group plc. The specimen is a commercial steel grade.

TABLE 1. Chemical composition of Y7N7 (in weight %).

Steel	C	Si	Mn	P	S	N	Nb	Ti	V
Y7N7	0.09	--	0.84	--	--	--	<0.005	0.001	--

To correlate steel microstructure to their mechanical properties, and particularly, with toughness a very good metallographic characterisation is performed.

Volume fraction of the carbides in the bainite, pearlite volume fraction and size distributions at the HAZ of Y7N7 steel at 1 mm from the fusion line, on T-sections, have been measured and characterised.

This section was etched with 2% nital for a few seconds, washed with ethanol and dried with hot air. The volume fractions of the different phases were measured using a point-count method on 12 fields (at × 400 magnification), as shown in Fig. 1.

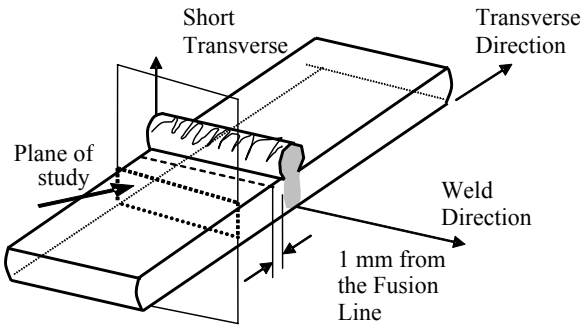

FIGURE 1. Micrographs obtained from the T-sections (plane of study).

The microstructure of base material is made up of ferrite-pearlite with a band structure along rolling direction, as observed in Fig. 2-a. The HAZ zone microstructure shows a structure of acicular ferrite, primary ferrite (FP) and Widmanstätten (FW), as shown in Fig.2-b. The measurements were realized according to the procedure of classification of the different phases proposed by Corus Group plc [3].

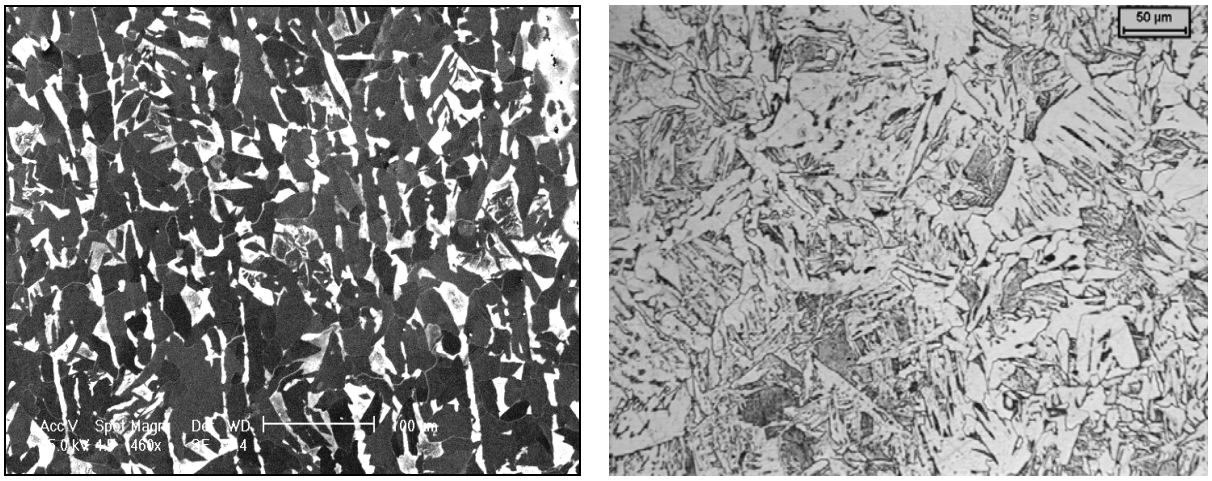

a) b)

FIGURE 2. Microstructure of Y7N7, a) Base material b) HAZ, at 1mm from the fusion line.

Tensile tests at 77, 156, 183 and 193K have been performed to determine the elastic limit (yield strength), ultimate tensile strength and hardening exponent of the base materials. Tensile specimens have been machined from the mid-thickness of the delivered plates. The geometry of the specimens is specified in Fig. 3.

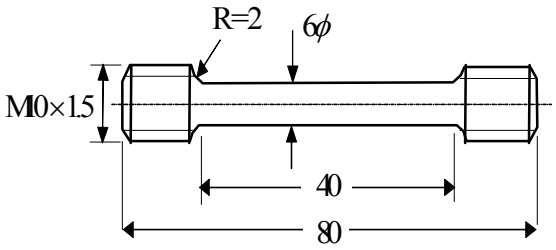

FIGURE 3. Tensile test-specimen geometry.

Tensile tests have been performed under displacement control at a fixed crosshead displacement rate of 0.5 mm/min., depending on the geometry of the specimen, to maintain a constant deformation rate.

Three-point bending samples, as shown in Fig. 4 were machined from the bead-in-groove welds. The plates containing these welds have been split into 20 mm strips.

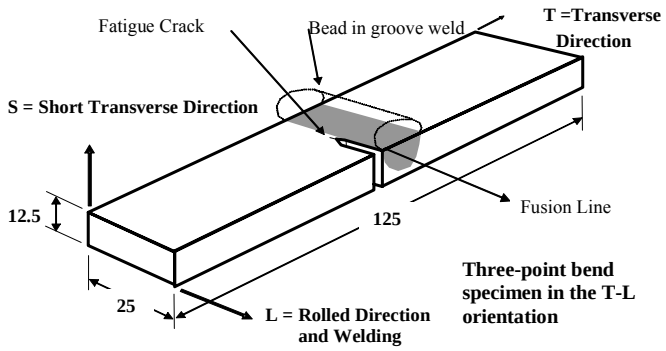

FIGURE 4. Schematic of the three-point bend specimen.

3PB tests have been carried out at the temperatures previously mentioned, to assure a brittle behaviour. Tests were performed submerging the test piece and fixtures in liquid nitrogen (77K), melting ethanol (156K) and melting acetone (183K and 193K). Temperature has been monitored using a thermocouple type K (Ni-Cr, Ni-Al). When needed, the displacement in the load line was recorded using a special device and an LVDT. Tests have been performed in displacement control at a fixed crosshead rate (0.6 mm/minute).

RESULTS AND DISCUSSION

Microstructural Characterisation

The obtained results of the characterization have been fitted to 4- or 3-parameter Gamma function according to Eq.1.

$$f(x)= \frac{c.a^{p}}{\Gamma(p)}.(x-d)^{cp-1}.e^{-a.(x-d)^{c}} \quad (1)$$

Table 2 shows the 3 or 4- parameter Gamma function fittings for the tested steel. Figures 5-6 summarise the fitting according to Eq.1.

TABLE 2. 3- or 4-parameter Gamma distribution function fits to the different microstructural components.

	Y7N7		
Steel	**Carbides**	**Pearlite**	**Matrix**
c	0.8	1.1	0.6
***a* (μm^{-n})**	6.311	10.035	1.5208
p	6.013	35.112	12.848
***d* (μm)**	0	0	0
f_v^*	0.072	0.0142	0.39

* Volume fraction of the different structural components.

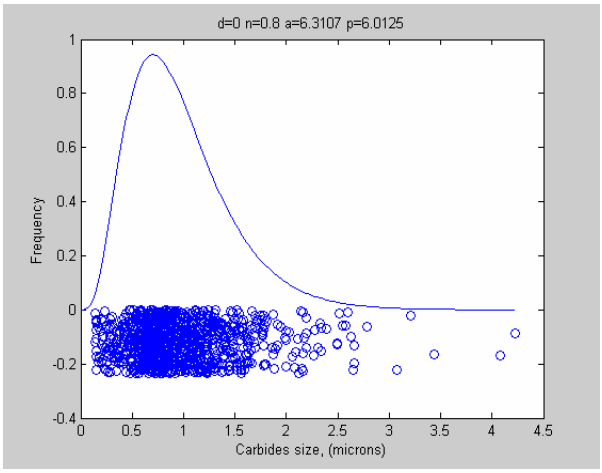

FIGURE 5. Y7N7, 3-parameter Gamma function for the carbides in the bainite.

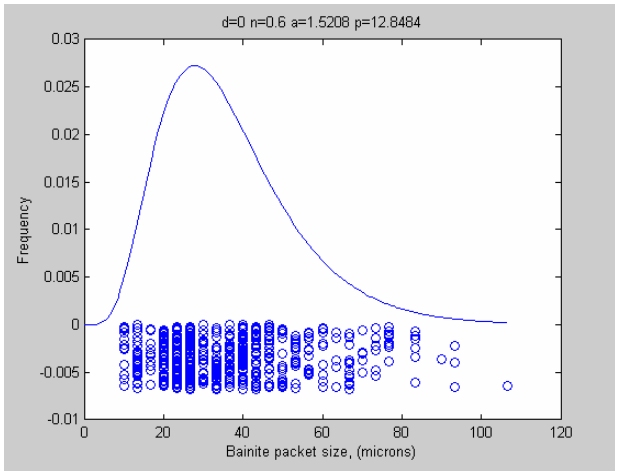

FIGURE 6. Y7N7, 3-parameter Gamma function for the bainite packet size.

Tensile Tests

As input data of the model, the yield strength and hardening exponent at the test temperature, fitting the base material behaviour to a Hollomon´s type Equation 2, have been introduced.

$$\sigma = \sigma_o \left(\frac{\varepsilon}{\varepsilon_o} \right)^n \tag{2}$$

The obtained results are summarized in Table 3. Load-displacement records for the Y7N7 steel at different temperatures can be observed in Figs. 7-10.

TABLE 3. Tensile tests at low temperatures.

Steel	*T* (K)	σ_y (MPa)	σ_{uts} (MPa)	σ_o Hollomon	nHollomon
Y7N7	77	755	780	384,79	0,0564
	156	345	511	190,52	0,2638
	183	340	502	177,29	0,2773
	193	325	509	176,34	0,2786

The yield strength of the HAZ has been estimated as 1.3 times that for the base material (after the hardness measurement profiles, measured through the weld into the base material) according to Eq. 3.

$$\sigma_{HAZ} = \frac{HV_{HAZ}}{HV_{BASE}} \cdot \sigma_O \tag{3}$$

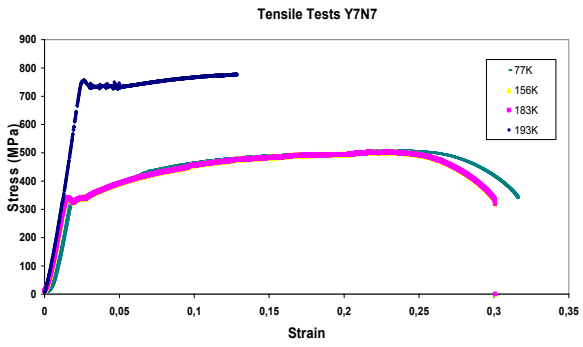

FIGURE 7. Engineering stress vs. engineering strain curve at different temperatures.

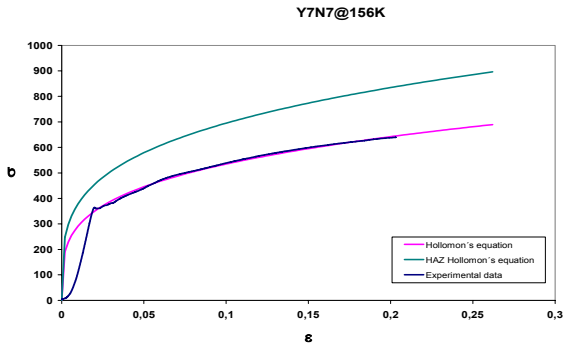

FIGURE 8. True stress vs. strain at 156K, and Hollomon´s fittings for base material and HAZ.

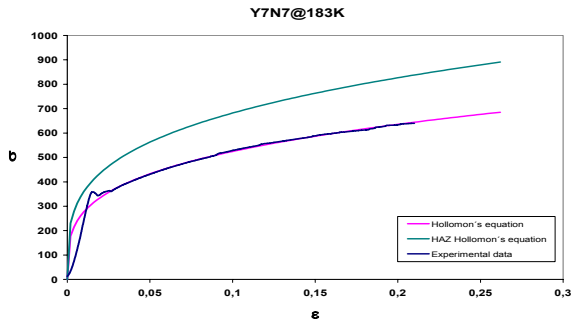

FIGURE 9. True stress vs. strain at 183K, and Hollomon´s fittings for base material and HAZ.

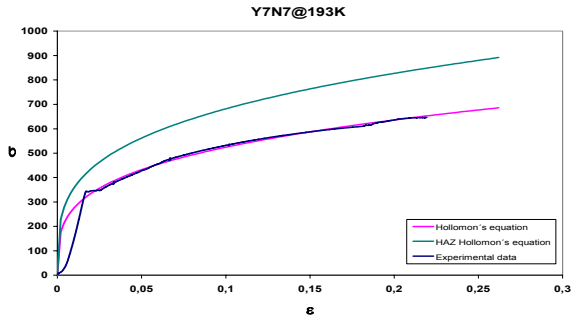

FIGURE 10. True stress vs. strain at 193K, and Hollomon´s fittings for base material and HAZ.

Fracture Mechanics Tests

The results of 3PB tests are illustrated in Fig. 11. In most cases, the plain strain condition is not satisfied (open symbols). The normal trend for fracture toughness, increasing with temperature, can be observed.

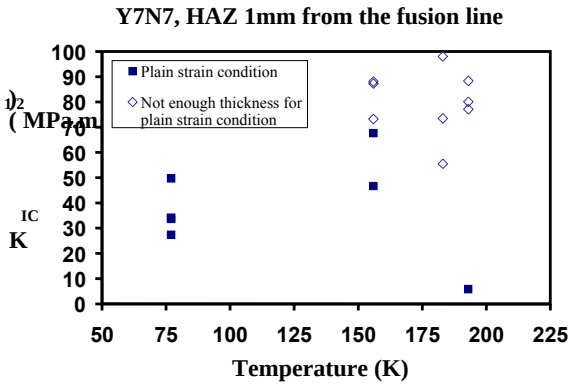

FIGURE 11. Fracture toughness vs. temperature for Y7N7.

Model description

A probabilistic model for brittle failure prediction from the HAZ based on microstructural data has been developed Martin-Meizoso *et al.* [4].The possibility for different populations of brittle particles in the microstructure is considered in the model Webster *et al.* [5], Moya-Gutiérrez *et al.* [6]

Two kind of particles or second phase are considered as triggers for nucleating the cleavage fracture: carbides from the bainite and pearlite.

The arresting stress intensity factors considered were the following: $K_{Ia}^{m/m}$ is the crack arrest ability at the boundaries of the bainitic packets, $K_{Ia}^{c/m}$ is the crack arrest ability at the carbide/bainite boundary, $K_{Ia}^{p/m}$ is the crack arrest ability at the pearlite/bainite boundary, $\alpha_{c/p}$ are the fracture probability of a particle (carbide or pearlite colony) of the mean size. Figures 12-14 show the obtained results for Y7N7 steel at the range 156K-193K. The values of $K_{Ia}^{p/m} = 2.5$ MPa√m and $\alpha_p = 0.000001$ are entered in the model.

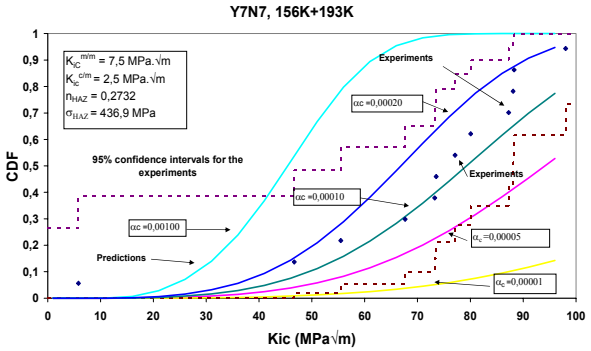

FIGURE 12. Effect of carbides as triggers for nucleating of cleavage fracture at the range 156K&193K.

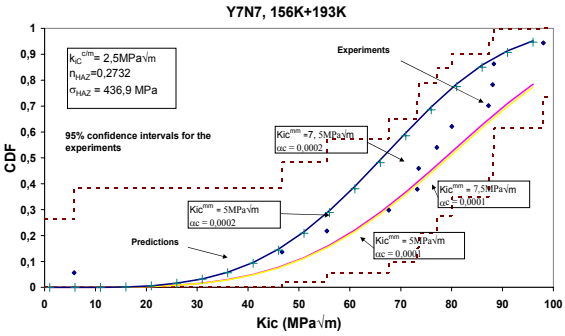

FIGURE 13. Effect of crack arresting ability at the boundaries of the bainite packets at 156K&193K.

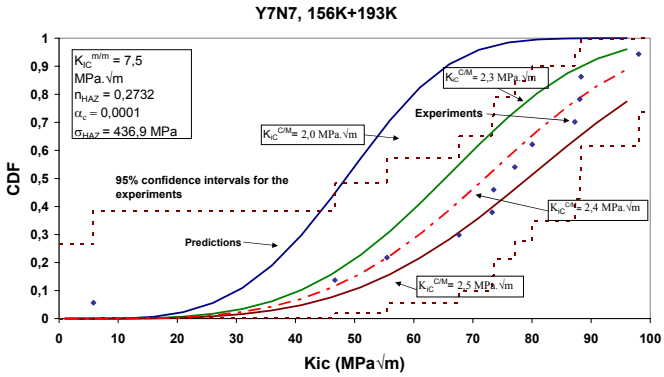

FIGURE 14. Effect of crack arresting ability at the carbide/bainite boundary at 156K&193K.

Conclusions

The model accounts for the effect of the temperature over the controlling factor of the toughness. The nucleation and the transmission of the microcrack to the neighbouring grain-packet across the particle/matrix interface is the controlling factor in the range between 156-193 K.

The matrix does not play any role as a controlling factor of the toughness. The carbides are the main crack-nucleation initiators for the tested steel.

Acknowledgments

This work has been developed within a ECSC project (7210.PR/245), coordinated by Corus plc. is gratefully acknowledged.

REFERENCES

1. Kim, B.C., Lee, S. Kim, N.J., and Lee, D.Y., "Microestructure and local brittle zone phenomena in High Strength Low Alloy Steel Welds", *Metallurgical Trans*. A, pp. 139-149 (1991).
2. Tweed, J. H., and Knott, J. F., "Mechanisms of failure in C-Mn Weld Metals", *Acta metall.* Vol. 35, No. 7, pp. 1401-1414 (1987).
3. Tewlis G, " Classification and Quantification of Microstructures in Steels", Report No. SL/PM/R/E7027/2/02/A, Corus Research, Development & Technology, Swiden Tecnology Centre, Feb. 2002, pA1/1.
4. Martin-Meizoso, A. Ocaña-Arizcorreta, I. Gil-Sevillano, J. and Fuentes-Pérez, M. "Modelling cleavage fracture of bainite steels", *Acta Metall. Mater.,* Vol 42, No. 6, pp. 2057-2068 (1994).
5. Webster, S. E*., et al*. "The prediction of HAZ microstructures and properties in structural steels", ECSC Contract no. 7210-PR/245, Report no. E7027-5 (ST) 022, Reference Source no. 108603,Corus Research, Development & Technology, Swinden Technology Centre Centre, February 2003.
6. Moya-Gutiérrez, C. Ocaña-Arizcorreta, I. and Martín-Meizoso, A. "Micromechanisms of cleavage fracture in HAZ of low C steel welds", In *Proceedings of the Fourth International Conference on Materials structure & Micromechanics of Fracture,* will be published in "*Material Science Forum",* December 2004.